EFFECTS OF DOUBLE-LEAKAGE TIP CLEARANCE FLOW ON THE PERFORMANCE OF A COMPRESSOR STAGE WITH A LARGE ROTOR TIP GAP

Chunill Hah
NASA Glenn Research Center,
MS 5-10, Cleveland, Ohio

Effects of a large rotor tip gap on the performance of a one and half stage axial compressor are investigated in detail with a numerical simulation based on LES and available PIV data. The current paper studies the main flow physics, including why and how the loss generation is increased with the large rotor tip gap. The present study reveals that when the tip gap becomes large, tip clearance fluid goes over the tip clearance core vortex and enters into the next blade's tip gap, which is called double-leakage tip clearance flow. As the tip clearance flow enters into the adjacent blade's tip gap, a vortex rope with a lower pressure core is generated. This vortex rope breaks up the tip clearance core vortex of the adjacent blade, resulting in a large additional mixing. This double-leakage tip clearance flow occurs at all operating conditions, from design flow to near stall condition, with the large tip gap for the current compressor stage. The double-leakage tip clearance flow, its interaction with the tip clearance core vortex of the adjacent blade, and the resulting large mixing loss are the main flow mechanism of the large rotor tip gap in the compressor. When the tip clearance is smaller, flow near the end wall follows more closely with the main passage flow and this double-leakage tip clearance flow does not happen near the design flow condition for the current compressor stage.
When the compressor with a large tip gap operates at near stall operation, a strong vortex rope is generated near the leading edge due to the double-leakage flow. Part of this vortex separates from the path of the tip clearance core vortex and travels from the suction side of the blade toward the pressure side of the blade. This vortex is generated periodically at near stall operation with a large tip gap. As the vortex travels from the suction side to the pressure side of the blade, a large fluctuation of local pressure forces blade vibration. Non-synchronous blade vibration occurs due to this vortex as the frequency of this vortex generation is not the same as the rotor. The present investigation confirms that this vortex is a part of separated tip clearance vortex, which is caused by the double-leakage tip clearance flow.

INTRODUCTION

It is well known that tip clearance flow generates a large portion of the overall aerodynamic loss in a compressor. When the size of the tip clearance is increased, efficiency drops even more and the stall margin deteriorates drastically. Although significant progress has been reported in flow measurement techniques, a complete mapping of the flow field in and around the compressor tip gap is not yet possible as the tip clearance flow occurs in a very small area. High frequency pressure transducers mounted on the casing give the instantaneous pressure field as the rotor passes. However, an accurate measurement of the velocity field near the end wall and inside the tip clearance is very difficult. Alternatively, computational fluid dynamics (CFD) has been widely applied to understanding the physics of tip clearance flow over the past 30 years (for example, Hah [1986], Hoying et al. [1999], Vo et al. [2005], Chen et al. [2008], Yamada et al. [2013], etc.). Tip clearance flow physics from the CFD simulation are direct results of the applied numerical

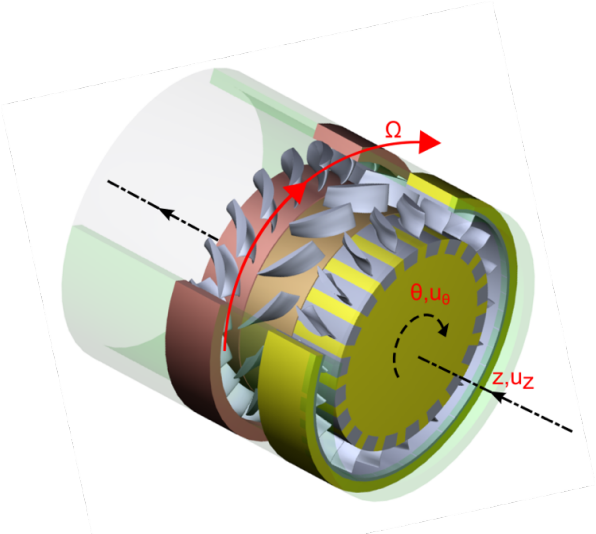

Figure 1: Cross section of the test compressor

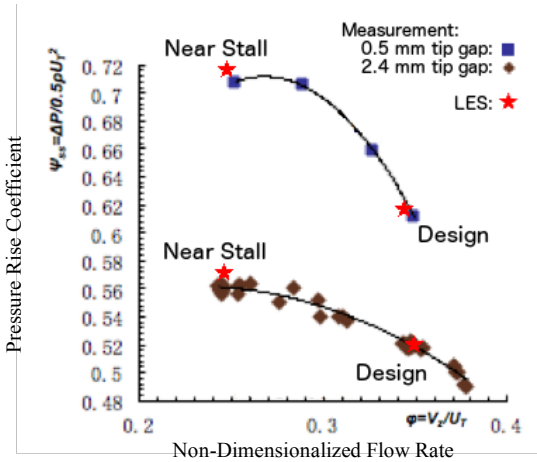

Figure 2: Pressure rise characteristics

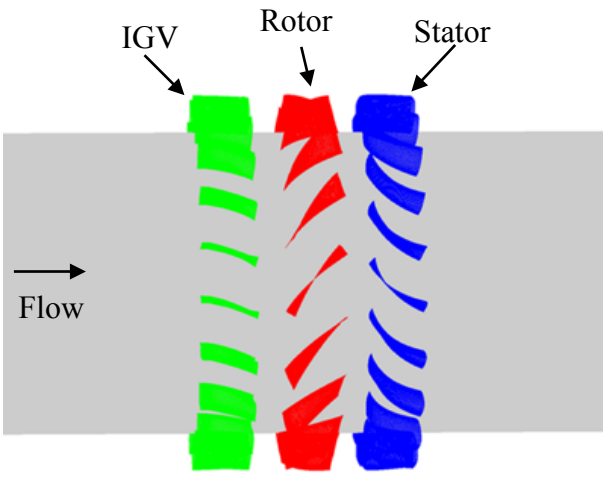

Figure 3: Computational domain

procedure (steady or unsteady, etc.) and the applied flow models. It appears that steady/unsteady Reynolds-averaged Navier-Stokes (RANS and URANS) simulation with current-generation turbulence models do not represent all the important tip clearance flow physics. Although the tip clearance flow originates from the simple pressure difference between the pressure side and the suction side of the blade at the rotor tip, the structure of the tip clearance flow and its interaction with the main passage flow are very complex and transient.

Effects of a large tip gap on compressor operation at near stall have been widely investigated (for example, Copenhaver et al. [1996], Mailach et al. [2000], Maerz et al. [2002], Inoue et al. [2004], etc.). Rotating instability and non-synchronous blade vibration occurs when the tip gap is increased in axial compressors. Maerz et al. [2002] reported movement of the instability vortex along the leading edge plane is the main cause of the instability during compressor operation at near stall operation. Inoue et al. [2004] and Yamada et al. [2013] reported the formation of a tornado-type vortex near the suction surface and subsequent vortex breakup as the main mechanism of the flow at near stall operation with a large tip gap. Fundamental flow mechanisms for the increased loss and the decrease of the stall margin with larger tip clearances in compressors have not been fully explained.

The present study is intended to examine the detailed development of tip clearance flow and its effects on compressor performance with a large tip gap (4 % of rotor span). The unsteady tip clearance flow from a Large Eddy Simulation (LES) based on a fine computational grid and available Particle Image Velocimetry (PIV) results in a low speed one and half stage axial compressor are examined in detail for this purpose.

ONE AND A HALF STAGE LOW SPEED AXIAL COMPRESSOR AND PIV FOR TIP CLEARANCE FLOW

A new program to investigate the unsteady tip clearance flow in a low speed one and a half stage axial compressor was initiated under the auspices of the NASA Fixed Wing Project to understand and mitigate losses associated with large rotor tip gaps of N+3 relevant small, high overall pressure ratio compressor aft stages. Detailed measurements of the unsteady tip clearance flows at two tip clearances (0.5 mm and 2.4 mm, which are 0.8 % and 4 % rotor span and 0.49 % and 2.3 % of rotor blade chord at tip) have been performed with three-dimensional PIV in an index-matched test facility at the Johns

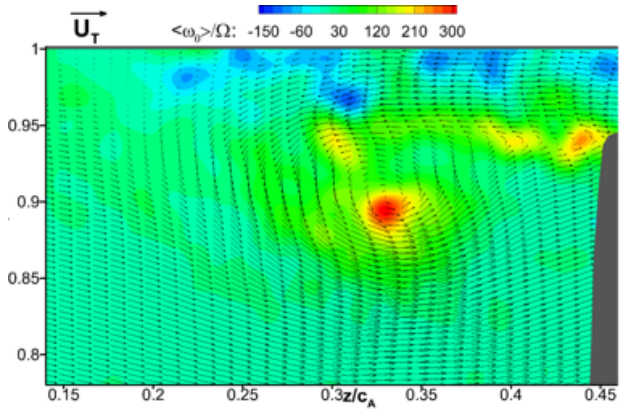

Figure 4(a): Instantaneous velocity vectors and vorticity distribution from PIV, 2.4 mm gap, design condition, 65.5% blade chord (Tan et al. [2014])

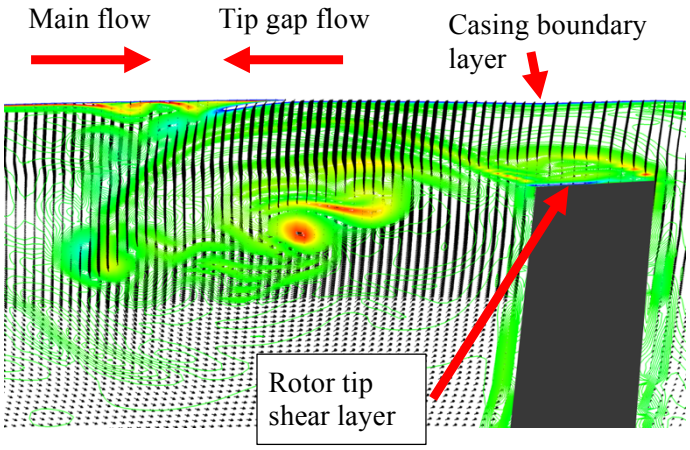

Figure 4(b): Instantaneous velocity vectors and vorticity distribution from LES, 2.4 mm gap, design condition, 65.5% blade chord

Hopkins University. Details of the PIV procedure are given by Wu et al. [2011].

One of the goals of the new program is to obtain a detailed velocity measurement inside the tip clearance. To measure unsteady velocity vectors inside the tip gap with an optical measurement technique, unobstructed access to the tip clearance with minimal optical reflection is required. For this purpose, the optically index matched test facility at Johns Hopkins University (JHU) was selected to perform the unsteady tip clearance flow measurement. A one and half stage compressor scaled from the NASA Glenn Research Center's Low-Speed Axial Compressor (LSAC) was designed to fit into the JHU test facility.

The design intent for the JHU compressor, which is focused on investigating the flow physics of the rotor tip clearance flow field, was to be an aerodynamically scaled derivative of the first one and one half stages (i.e., inlet guide vane, rotor, and stator) of the NASA Glenn Research Center's Low-Speed Axial Compressor (LSAC), which comprises an IGV followed by four geometrically identical stages designed for an accurate low-speed simulation of a high-speed multistage core compressor (Wasserbauer [1995]). In addition, commensurate with the NASA LSAC compressor, the JHU compressor has a long entrance length to develop thick endwall boundary layers typical of an embedded stage. The target Reynolds number is 4.0×10^5 based on the tip speed and the rotor chord length at the tip. Details of the JHU compressor design parameters are given by Hah et al. [2014].

The compressor test section is given in Figure 1. The compressor static pressure rise characteristic curves for two tip gaps are given in Figure 2. Static pressure rises from LES at the four operating conditions are marked in Figure 2. As shown in Figure 2, the compressor performance deteriorates substantially with the larger tip gap. Calculated and measured flows at the design and near stall conditions with the 2.4 mm tip gap are compared with those of the 0.5 mm gap and analyzed in detail to identify responsible flow mechanisms of aerodynamic loss generation.

NUMERICAL PROCEDURE

A LES was applied in the present study to calculate the unsteady flow and various vortex structures in the rotor tip gap. With spatially-filtered Navier-Stokes equations, the subgrid-scale stress tensor term needs to be modeled properly for closure of the governing equations. A Smagorinsky-type eddy-viscosity model was used for the subgrid stress tensor, and the standard dynamic model by Germano et al. [1991] was applied.

In the current study, the governing equations are solved with a pressure-based implicit method using a fully conservative control volume approach. A third-order accurate interpolation scheme is used for the discretization of convection terms and central differencing is used for the diffusion terms. For the time-dependent terms, an implicit second-order scheme is used and a number of sub-iterations are performed at each time step. Approximately 6000 time steps are used for one rotor revolution.

Standard boundary conditions for the multi-blade rows were applied at the boundaries of the computational domain (Hah and Shin [2012]). The inflow boundary of the computational domain was located 20 average blade heights upstream of the rotor leading edge in order to dampen out any possible reflections. Likewise, the outflow boundary was located 20 blade heights downstream from the trailing edge. Circumferentially averaged static pressure at the exit boundary casing was specified to control the mass flow rate. Non-reflecting boundary conditions were applied at the inlet and exit boundaries.

The current compressor stage has 20 IGV blades, 15 rotor blades, and 20 stator blades. A full annulus LES was

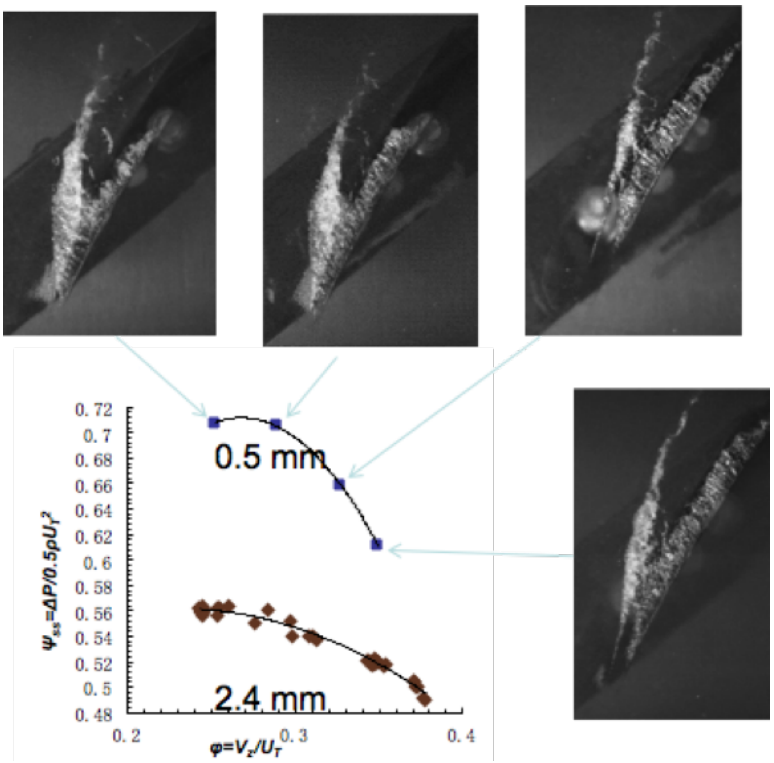

Figure 5(a): Cavitation tip clearance vortex visualization, 0.5 mm tip gap (Tan et al. [2014])

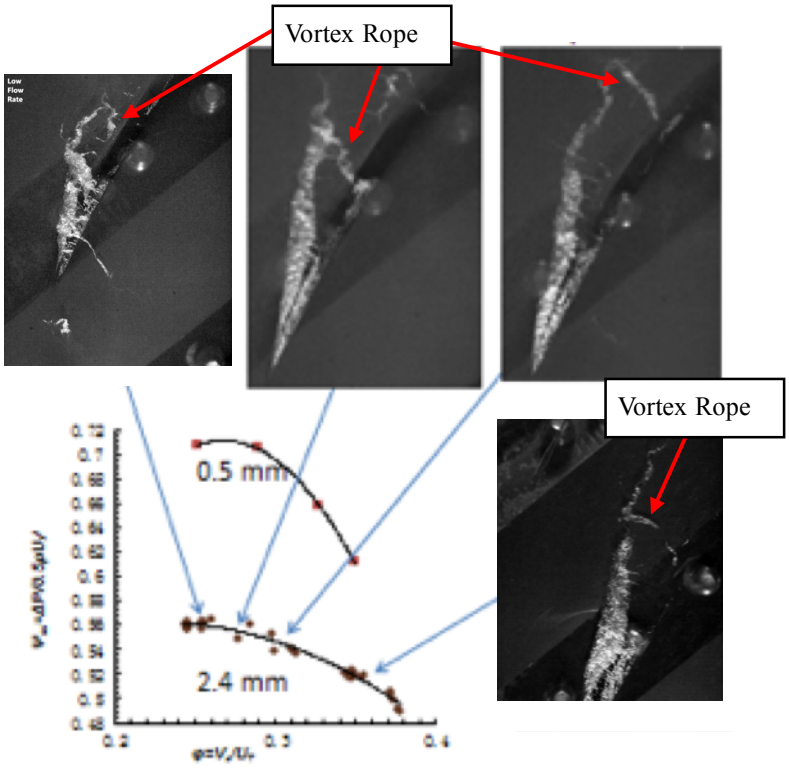

Figure 5(b): Cavitation tip clearance vortex visualization, 2.4 mm tip gap (Tan et al. [2014])

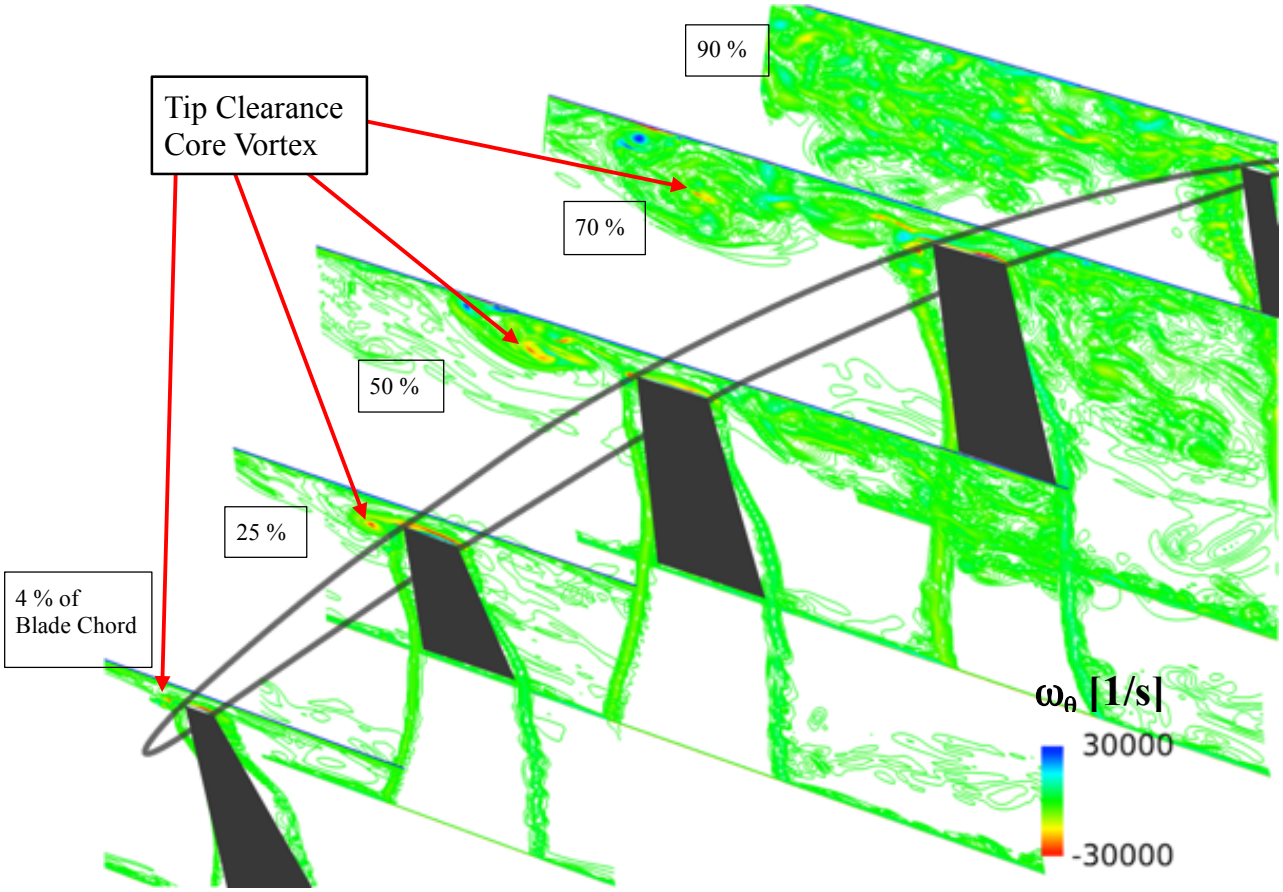

Figure 6: Instantaneous vorticity distribution at meridional planes, 2.4 mm tip gap, design condition

performed for the flows at near stall condition. A simulation with a reduced blade count with 4-3-4 blades with a finer CFD grid were applied to study the detailed flow structure at the design condition and near stall. The computational grid for the 4-3-4 blade case was 400 nodes for IGV and stator and 760 nodes for the rotor in the blade-to-blade direction, 480 nodes in the spanwise direction, and 450 nodes in the streamwise direction for each blade passage. The rotor tip clearance geometry is represented by 120 nodes inside the tip gap in an attempt to accurately resolve the tip clearance flow field. For the full annulus simulation, the numerical grid was reduced to 200 nodes in the blade-to-blade direction and 200 nodes in the spanwise direction with 60 nodes inside the tip gap. I-grid topology is used to reduce grid skewness and a single-block grid is used. The grid size for the entire one and half stage is about 980 million nodes for both the 20-15-20 and 4-3-4 simulations. The wall resolution is within the range $Dx^+ < 10$, $Dy^+ < 1.0$, and $Dz^+ < 1.5$ in streamwise, pitchwise, and spanwise directions. Figure 3 shows the computational domain of the compressor stage.

All the computations were performed with NASA's Columbia supercomputing system, which allows parallel computation with up to 512 processors.

GENERATION AND TRANSPORT OF TIP CLERANCE CORE VROTEX AND TIP CLERANCE FLOW WITH THE LARGE TIP GAP

Figure 4 compares instantaneous velocity vectors and vorticity contours at the meridional plane located 65.5 % chord downstream from the leading edge between the LES and PIV measurements for the 2.4 mm tip gap. Three-dimensional SPIV measurements were performed at various merdional planes (Tan et al. [2014]) and LES results were also interpolated on the corresponding measurement planes for the comparison. As shown in Figure 4, the tip corner geometry of the test compressor is slightly different due the manufacturing process of the test model. However, the overall measured tip flow structure agrees fairly well with the LES. Further comparisons between PIV measurements and LES for two gaps at various axial locations are given by Hah et al [2015].

The instantaneous vorticity distribution from the LES in Figure 4 reveals that the tip clearance vortex is formed by the

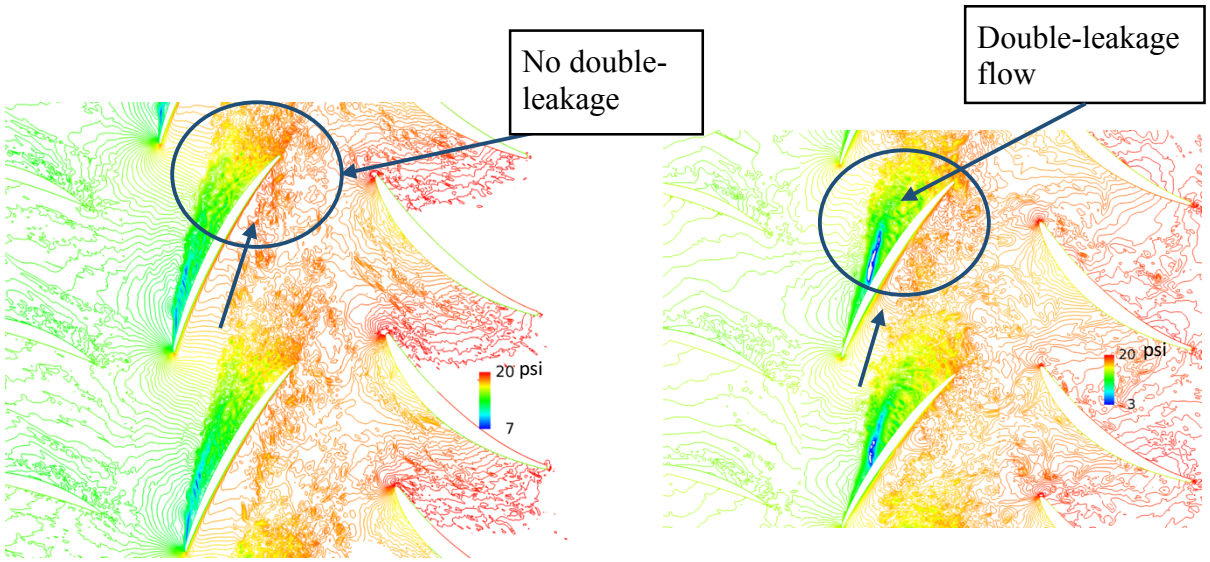

0.5 mm tip gap

2.4 mm tip gap

Figure 7: Instantaneous pressure at rotor tip section, design condition

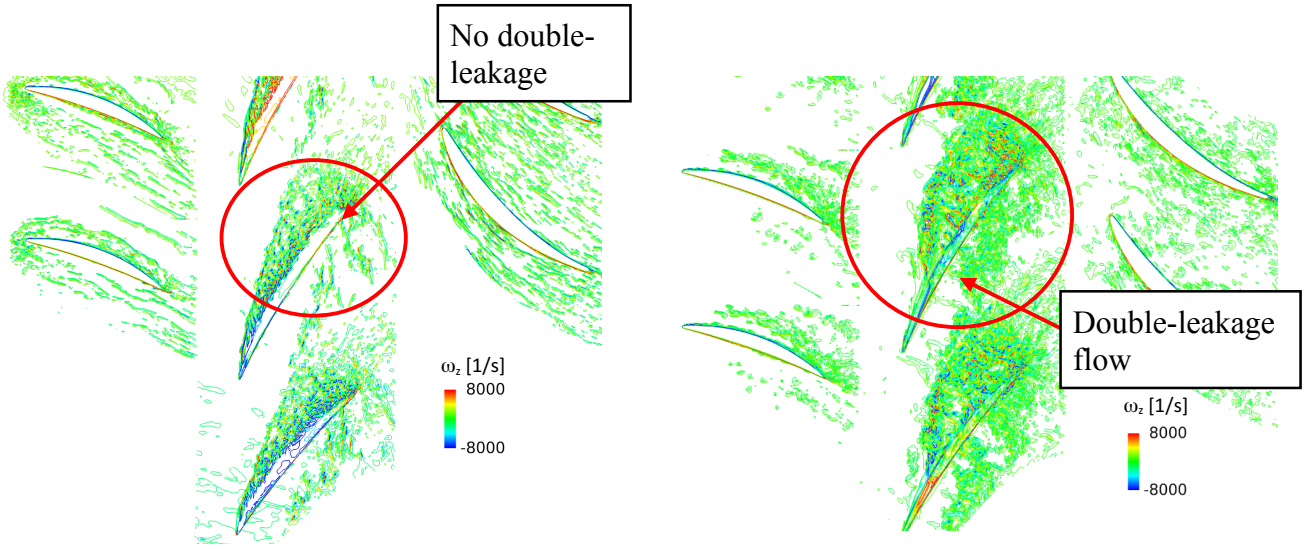

0.5 mm tip gap

2.4 mm tip gap

Figure 8: Instantaneous distribution of vorticity, design condition

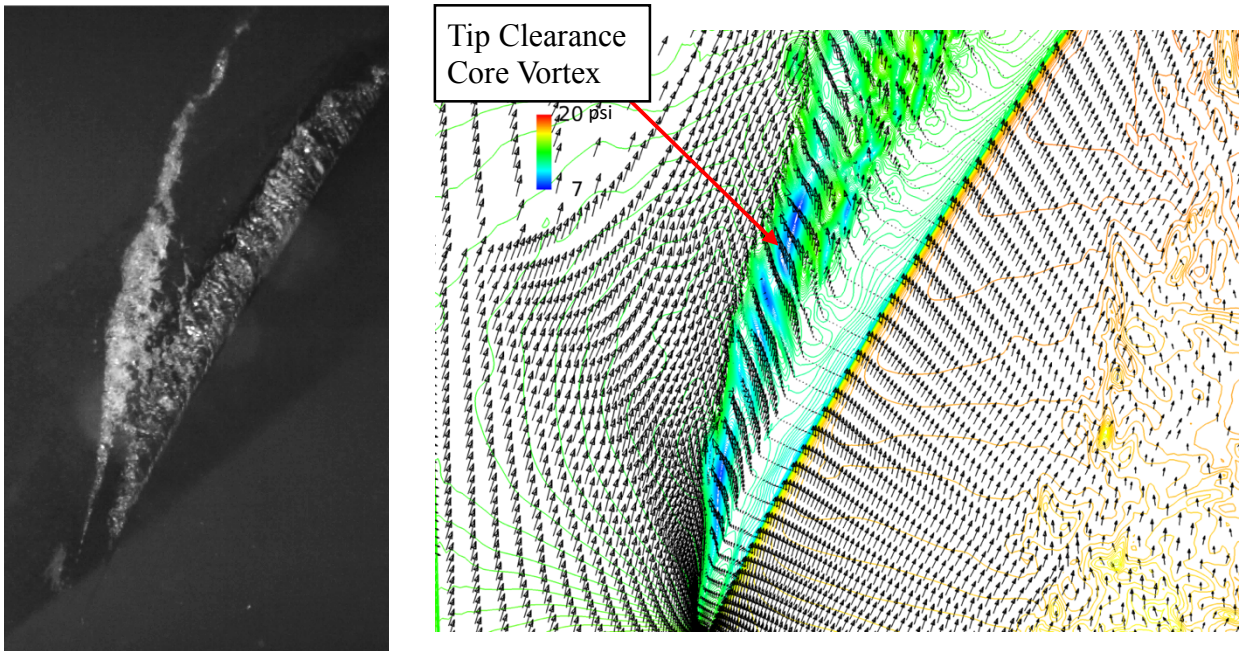

Flow Visualization LES

Figure 9: Tip clearance flow structure, 0.5 mm tip gap, design condition

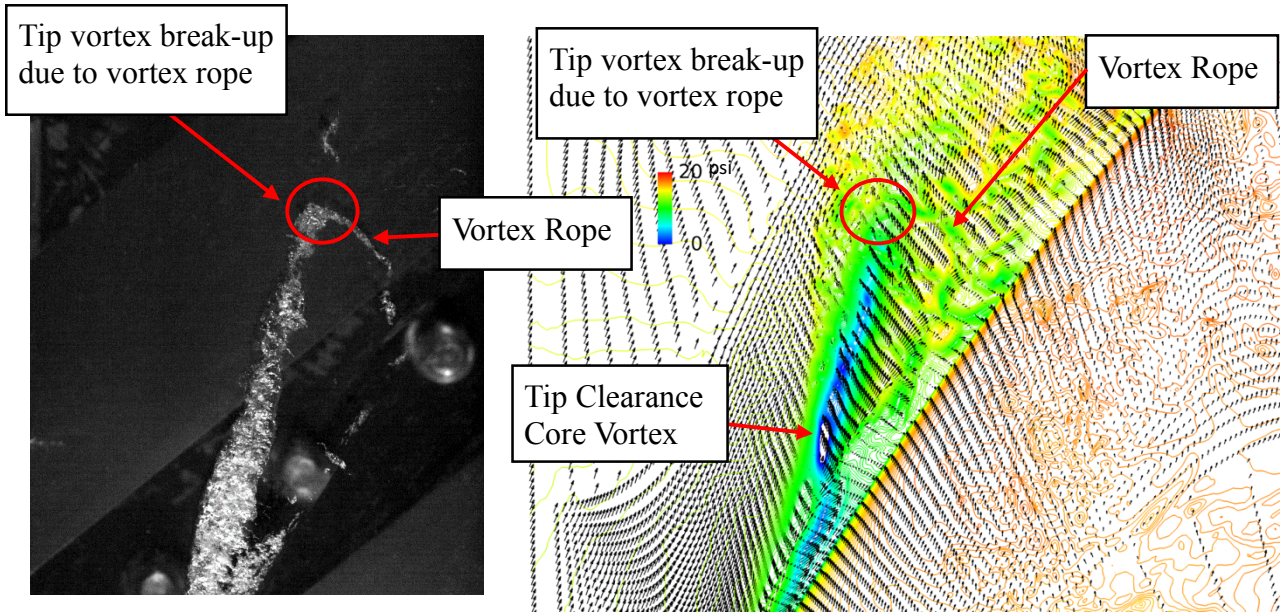

Flow Visualization LES

Figure 10: Tip clearance flow structure, 2.4 mm tip gap, design condition

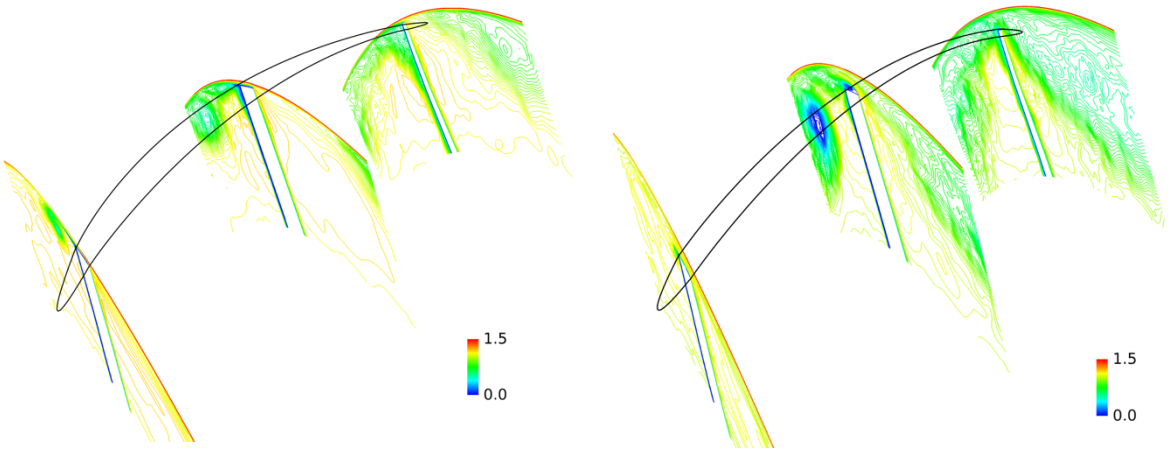

0.5 mm tip gap 2.4 mm tip gap

Figure 11: Instantaneous relative non-dimensional total pressure distribution, design condition

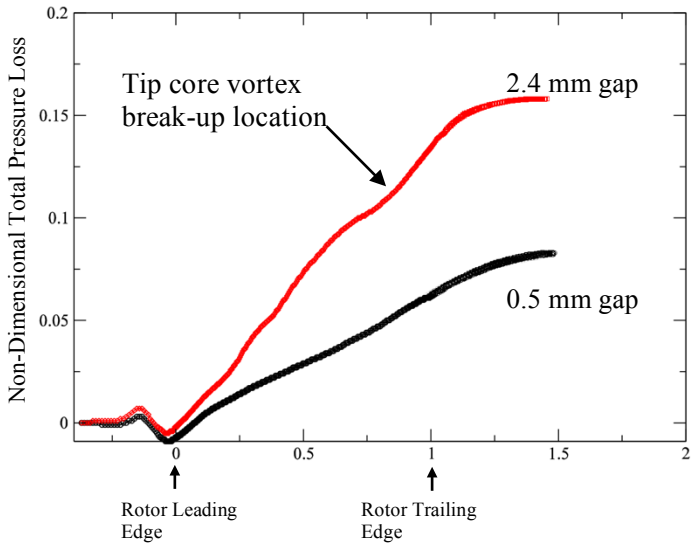

Figure 12: Comparison of total pressure loss development

shear layers on the rotor tip and compressor casing. When these shear layers collide with the incoming main flow, these shear layers are turned radially inward and form the tip clearance core vortex. The tip clearance vortex is formed by the thin shear layers on the rotor tip and the casing and not by the main tip gap flow itself.

Visualizations of instantaneous tip clearance vortices from the cavitation inception are compared in Figure 5 for the two tip gaps. Cavitation inception occurs at areas with low local static pressure and provides a qualitative indication of the tip vortex development. Tip vortex visualizations in Figure 5 show that a vortex rope with low pressure is formed with the large tip gap. The main tip vortex structure seems to be broken up by this vortex rope. Instantaneous vorticity contours at five meridional planes from the LES for the large tip gap at the design condition are given in Figure 6. The tip clearance core vortex is formed very close to the leading edge. The tip clearance flows further downstream of the leading edge and rolls up around the core vortex as it feeds up the circulation. Instantaneous vorticity contours in Figure 6 show that the tip clearance core vortex becomes completely broken-up after about 80 % of the axial chord, which is also shown in the tip vortex visualization in Figure 5. The tip clearance vortex visualization in Figure 5(a) shows that the sudden break-up of the tip clearance core vortex does not occur with the 0.5 mm gap except at near stall condition.

DOUBLE-LEAKAGE TIP CLEARANCE FLOW WITH THE LARGE TIP GAP

Instantaneous pressure fields at the rotor tip section from the LES at the design condition are compared in Figure 7. The LES shows clearly that a vortex rope is formed with the 2.4 mm tip gap and the tip clearance core vortex is broken-up when the vortex rope intersects the tip clearance core vortex. With the small tip gap (0.5 mm), the vortex rope does not develop and the tip clearance core vortex is transported downstream without forced break-up. The instantaneous radial component of the vorticity at the middle of the tip gap is compared in Figure 8. With the small tip gap, tip clearance flow originating downstream of the leading edge wraps up around the tip clearance core vortex and does not reach the adjacent blade. On the other hand, tip clearance flow originating from the rear part of the rotor tip gap flow over the tip clearance core vortex and gets into the tip gap of the adjacent blade with the large tip gap. When this double-leakage flow interacts with the tip clearance flow of the adjacent blade, the vortex-to-vortex interaction creates the vortex rope. In Figures 9 and 10, instantaneous velocity vectors at 1 % of the tip gap height are compared at the design condition. For the 0.5 mm tip gap, velocity vectors above the rotor tip have almost identical direction and seem to be driven

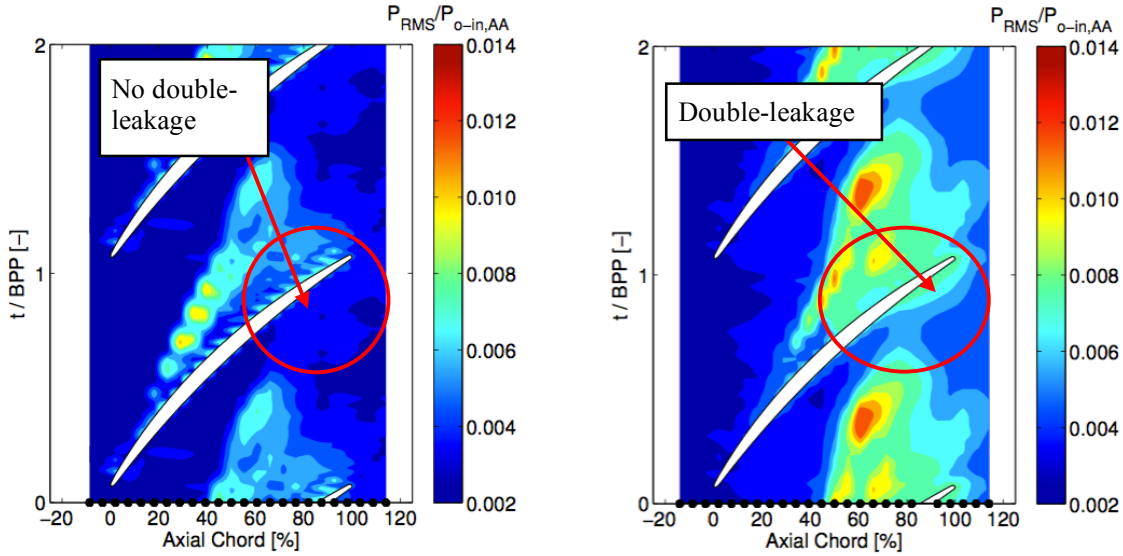

Figure 13: Casing pressure unsteadiness of two tip gaps in a high speed compressor (Berdanier and Key [2015])

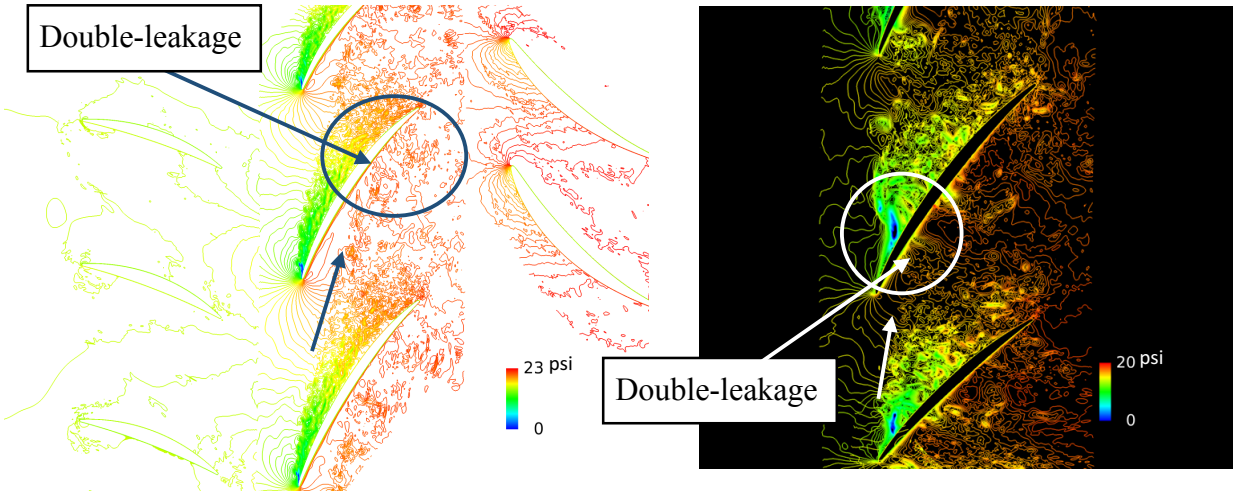

Figure 14: Instantaneous distribution of static pressure at rotor tip section, near stall condition

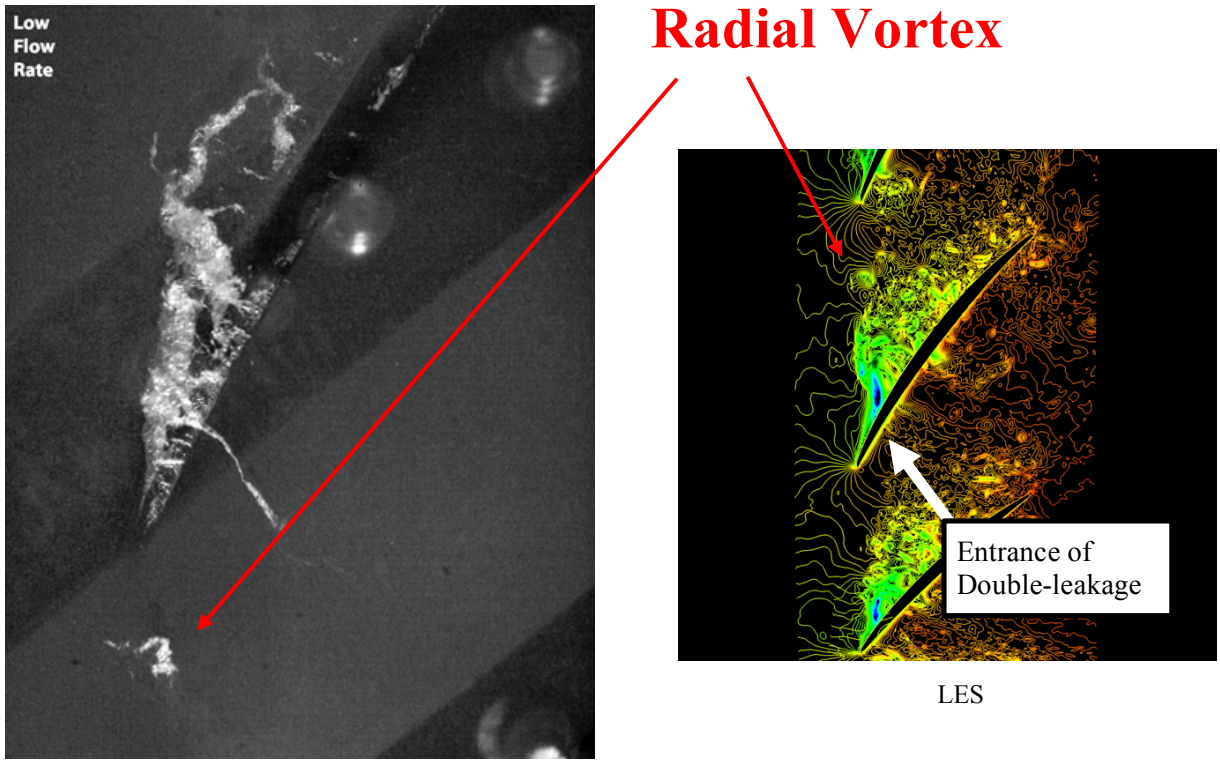

Figure 15: Comparison of tip clearance flow structure, 2.4 mm tip gap, near stall

by the pressure difference across the blade. For the 2.4 mm tip gap, velocity vectors above the rotor tip show strong vortex interactions, which leads to the vortex rope development.

The double-leakage tip clearance flow occurs when the tip gap is increased and the vortex rope is created due to the vortex interaction between tip clearance flows from the two adjacent tip gaps. The vortex break-up due to the vortex rope is one of the main mechanisms of the large loss generation with a large tip gap. With the sudden break-up of the tip clearance vortex, additional loss is generated due to the large mixing.

Sirakov and Tan [2003] investigated the effects of rotor double-leakage tip clearance flow interaction. They found that double-leakage tip clearance flow typically occurs at higher loading and additional loss due to the double-leakage can be as high as half of the total loss generation from the tip clearance flow. The present work reveals that the double-leakage tip clearance flow can occur at all flow ranges when the tip gap is increased. Figure 11 compares the instantaneous distribution of relative total pressure at the design condition of the two tip gaps. In Figure 11, the total pressure at the rotor inlet was used for the non-dimensional value. Significantly larger loss generation is observed with the 2.4 mm tip gap, especially after the vortex break-up. Axial development of the relative total pressure loss is compared in Figure 12 for the two tip gaps. The relative total pressure loss in Figure 12 is mass-averaged at each axial location and non-dimensionalized with the inlet dynamic head. In Figure 12, the location where the tip core vortex break-up occurs due to the interaction with the vortex rope is indicated. Increased loss generation from the core vortex break-up is shown with the change of slope. The total pressure loss is about 3 times greater with the 2.4 mm gap than that of the 0.5 mm gap.

The double-leakage tip clearance flow was also observed at the design flow condition in a high speed multi-speed axial compressor when the tip gap is increased (Berdanier and Key [2015]). RMS of the wall static pressure over the first stage rotor for two tip gaps (1.5 % and 4.0 % of rotor span) at the design flow condition are shown in Figure 13. Unsteadiness in the static pressure increases toward the trailing edge of the adjacent blade when the tip gap is increased from 1.5 % to 4.0 %. This increased unsteadiness of the static pressure near the casing happens as the tip clearance flow travels over the tip clearance core vortex and reaches the adjacent blade, causing the double-leakage tip clearance flow.

Many casing treatments to control the compressor casing flow have been designed and applied without a full understanding of the actual flow field near the end wall and inside the tip clearance. Some new casing treatment ideas, which can control the double-leakage of the tip clearance flow, might be able to achieve higher efficiency, even at the

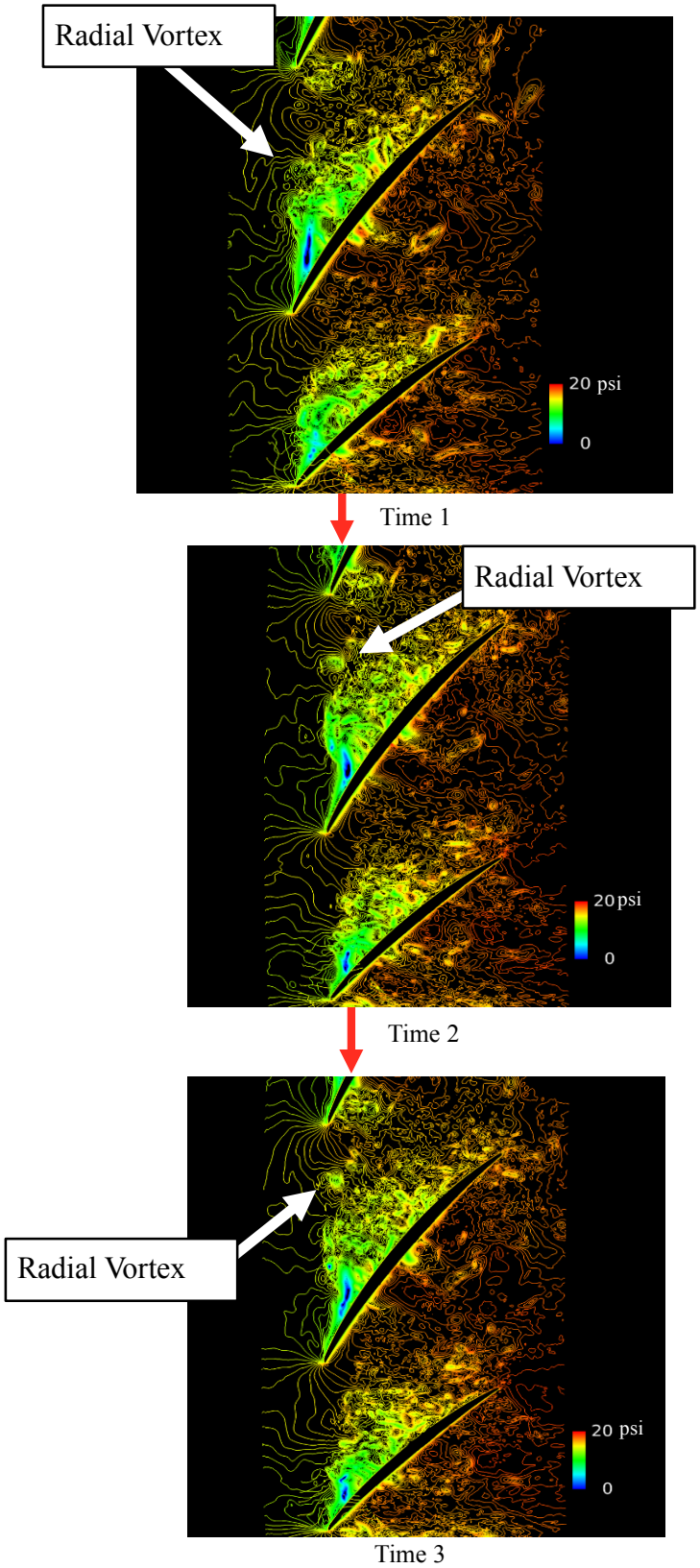

Figure 16: Movement of radial vortex, 2.4 mm tip gap, near stall condition

design condition, for compressors operating with a large rotor tip gap.

DOUBLE-LEAKAGE TIP CLEARANCE FLOW AND FLOW INSTABILITY AT NEAR STALL OPERATION

Instantaneous pressure distributions at the rotor tip section at near stall operation from the LES are given for two tip gaps in Figure 14. The instantaneous pressure distribution in Figure 14 shows that the tip clearance core vortex is broken up abruptly near the leading edge with the 2.4 mm tip gap while the tip core vortex extends much longer with the 0.5 mm tip gap. With the 2.4 mm tip gap, the vortex rope is formed close to the leading edge, where the front of the double-leakage flow enters the adjacent blade, and this vortex rope breaks up the tip clearance core vortex of the adjacent blade. Detailed tip flow structures with the 2.4 mm tip gap at near stall operation are compared in Figure 15. The unsteady pressure field from the LES and the cavitation flow visualization at various times show that shear layers on the compressor casing travel over the trajectory of the tip clearance core vortex and form a radial vortex structure. This radial vortex is shown both in the flow visualization and in the LES in Figure 15. This radial vortex travels from the suction side of the blade to the pressure side of the blade. The movement of this vortex is shown in Figure 16 with the full annulus flow simulation. This moving vortex has a lower pressure core and it is generated intermittently, creating an oscillating pressure field near the leading edge. This phenomenon has been identified as non-synchronous blade vibration at near stall operation. This radial vortex has been identified as an instability vortex, or shed vortex, by previous studies (Maerz et al [2002], Kielb et al. [2003]). The current study confirms that this moving instability vortex originates from the rotor tip clearance flow and is a part of the tip clearance vortex with a large tip gap. This phenomenon occurs only with a large tip gap at the near stall stable operation. This instability vortex is not the same radial vortex near the casing during the stall inception, which some previous studies indicated that it originates from the flow separation near the mid-span (Yamada et al. [2013], Pullan et al. [2013], and Weichert and Day [2013]).

CONCLUDING REMARKS

Effects of double-leakage tip clearance flow in a compressor stage are investigated with a fine-grid LES and available PIV measurements. Following are the two main findings from the current investigation:

1. When the clearance is increased from 0.8 % of the rotor span (0.5 mm tip gap) to 4 % of the rotor span (2.4 mm tip gap), double-leakage of the tip clearance flow occurs at all operating conditions from the design condition to near stall operation. When the double-leakage tip clearance flow enters into the tip gap of the adjacent blade, a vortex rope is formed

due to the vortex-to-vortex interaction. This vortex rope breaks up the tip clearance core vortex of the adjacent blade when the vortex rope collides with it. Additional mixing loss due to this vortex break-up is the main mechanism of the large aerodynamic loss with the large tip gap. Some casing treatment concepts might be able to increase the performance of compressor with a large rotor tip gap, even at near design operation, by controlling the double-leakage tip clearance flow. The current study reveals that the tip clearance core vortex is formed when thin shear layers on the rotor tip and the casing are turned radially inward when they collide with the incoming main flow.

2. When the compressor with a large rotor tip gap operates at near stall condition, vortex break-up occurs close to the leading edge as the double-leakage tip flow enters the tip gap very close to the leading edge. At near stall operation with a large rotor tip gap, a radial vortex is formed as the vortex rope breaks up the tip clearance core vortex, which travels from the suction side to the pressure side of the blade. This radial vortex is part of the tip clearance vortex formed by the thin shear layers on the casing and the rotor tip. This traveling radial vortex occurs at near stall operation only with the large tip gap. This radial vortex is not the same radial vortex that originates from flow separation near mid-span during the initial stall inception.

ACKNOWLEDGMENTS

The author gratefully acknowledges the support of this work by the NASA Fundamental Aeronautics program, Fixed Wing Project. Many useful discussions with Professor J. Katz of the Johns Hopkins University and Michael Hathaway of NASA Glenn are greatly appreciated.

REFERENCES

Berdanier, R. A. and Key N.L., 2015, "Characterization of tip leakage flow trajectories in a multistage compressor using time-resolved over-rotor static pressure," ISABE paper, ISABE-2015-20006.

Chen, J.P., Hathaway, M.D., and Herrick, G.P., 2008, "Prestall Behavior of a Transonic Axial Compressor Stage via Time-Accurate Numerical Simulation," ASME Journal of Turbomachinery, Vol. 30, October 2008.

Copenhaver, W.W., Mayhew, E.R., Hah, C., and Wadia, A.R., 1996, "The Effect of Tip Clearance on a Swept Transonic Compressor Rotor," ASME J. of Turbomachinery, Vol. 118, pp. 230-239.

Germano, M., Piomelli, U., Moin, P., and Cabot, W. H., 1991, "A Dynamic Subgrid-Scale Eddy-Viscosity Model," Journal of Fluid Mechanics, Vol. A3, pp. 170-176.

Hah, C., 1986, "A Numerical Modeling of Endwall and Tip-Clearance- Flow of an Isolated Compressor," ASME Journal of Engineering for Gas Turbines and Power Vol. 108, No. 1, pp. 15-21.

Hah, C. and Shin, H., 2012, "Study of Near –Stall Flow Behavior in a Modern Transonic Fan with Compound Sweep," ASME Journal of Fluids Engineering, Vol.134, pp.071101-071107.

Hah, C., Hathaway, M., and Katz, J., 2014, "Investigation of Unsteady Flow Field in a Low Speed One and a Half Stage Axial Compressor: Effects of Tip Gap Size on the Tip Clearance Flow Structure at Near Stall Operation," ASME paper GT2014-27094.

Hah, C., Hathaway, M., and Katz, J., 2015, "Investigation of Unsteady Tip Clearance Flow in a Low Speed One and Half Stage Compressor with PIV and LES," ASME paper AJKFluids2015-02061.

Hoying, D.A. Tan, C.S., Vo, H.D., and Greitzer, E.M., 1999, "Role of blade passage flow structure in axial compressor rotating flow inception," ASME J. of Turbomachinery, 121,pp.735-742.

Inoue, M., Kuromaru, M, Yoshida, S., Minami, T., Yamada, K., and Furukawa, M., 2004, "Effects of Tip Clearance on Stall Evolution Process in a Low-Speed Axial Compressor Stage," ASME Paper GT2004-5335.

Kielb, R. E., Barter, J. W., Thomas, J., and Hall, K. C., 2003, "Blade Excitation by Aerodynamic Instabilities–A Compressor Blade Study," ASME Paper GT2003-38634.

Maerz, J., Hah, C., and Neise, W, 2002, "An Experimental and Numerical Investigation into the Mechanism of Rotating Instability," ASME Journal of Turbomachinery, Vol. 124, pp. 367-375.

Mailach, R., Lehmann, I., and Vogeler, K., 2000, "Rotating Instabilities in an Axial Compressor Originating from the Fluctuating Blade Tip Vortex," ASME Paper 2000-GT.

Pullan, G., Young, A.M., Day, I.J., Greitzer, E.M., Spakovszky, Z.S., 2013, "Origins and Structure of Spike-Type Rotating Stall," ASME paper 2012-68707.

Sirakov, B.T. and Tan, C., 2003, "Effects of Unsteady Stator Wake-Rotor Double-Leakage Tip Clearance Flow Interaction on Time-Average Compressor Performance", ASME Journal of Turbomachinery, Vol. 125, pp.465-474.

Tan, D., Yuanchao, L., Wilkes, I., Miorini, R.L., and Katz, J., 2014, "Visualization and Time Resolved PIV Measurements of the Flow in the Tip region of a Subsonic Compressor Rotor," ASME Paper GT2014-27195.

Vo, H. D., Tan, C. S., and Greitzer, E. M., 2005, "Criteria for Spike Initiated Rotating Stall," ASME Paper GT2005-68374.

Wasserbauer, C. A., Weaver, H. F., and Senyitko, R. G., "NASA Low-Speed Axial Compressor for Fundamental Research," NASA TM 4635, Feb. 1995.

Weichert, S. and Day, I, 2013, “Detailed Measurements of Spike Formation in an Axial Compressor,” ASME paper GT2013.
Wu, H., Tan, D., Miorini, R.L., and Katz, J., 2011, “Three-Dimensional Flow Structures and Associated Turbulence in the Tip Region of a Water Jet Pump Rotor,” Exp. Fluids, 51(6), pp. 1721-1737.
Yamada, K, Kikuda, H., Furukawa, Kunjishima, S., and Hara, Y., 2013, “Effects of Tip Clearance on the Stall Inception Process in an Axial Compressor Rotor,” ASME Paper GT-2013-95479.